



Autophagy Suppression Accelerates Apoptosis Induced by Norcantharidin in Cholangiocarcinoma

Yun Wang^{1,2} · Wangjie Jiang¹ · Cunjiang Li³ · Xuanxuan Xiong⁴ · Hao Guo² · Qingzhong Tian² · Xiangcheng Li¹

Received: 10 February 2019 / Accepted: 13 August 2019 / Published online: 14 October 2019
© Arányi Lajos Foundation 2019

Abstract

Norcantharidin is a cantharidin demethylated analog with antitumor effects in many tumors, including cholangiocarcinoma. Autophagy suppression is known to increase chemosensitivity in cholangiocarcinoma. This study aimed to determine whether autophagy suppression accelerates apoptosis induced by norcantharidin in human cholangiocarcinoma cells. The human cholangiocarcinoma cell line QBC939 was incubated in RPMI 1640 medium with or without norcantharidin. Autophagy was induced using HBSS media with Ca^{2+} and Mg^{2+} supported by 10 mM HEPES or suppressed by treatment with 3-MA or transfection with siRNA against Atg5. The comparison was drawn between these conditions in mitochondrial membrane potential disturbance, the levels of reactive oxygen species (ROS), apoptotic proteins, and apoptosis. Cholangiocarcinoma cell apoptosis was accelerated by norcantharidin. Autophagy suppression up-regulated norcantharidin's pro-apoptotic effect, but autophagy induction weakened it. As apoptosis was accelerated, ROS production was up-regulated. Bax protein expression, cytochrome c levels and localization, mitochondrial membrane disturbance, and the levels of caspase-9, caspase-3, and cleaved PARP were higher when autophagy was suppressed, and all of those were down-regulated when autophagy was induced. To sum up, it was found that norcantharidin induced cholangiocarcinoma cell death, and autophagy suppression enhanced the pro-apoptotic action of norcantharidin, which appears to involve the mitochondrial apoptosis pathway activation and ROS generation.

Keywords Autophagy · Norcantharidin · Cholangiocarcinoma · Apoptosis

Yun Wang, Wangjie Jiang, Cunjiang Li and Xuanxuan Xiong contributed equally to this work.

✉ Xiangcheng Li
drxcli@njmu.edu.cn

¹ Key Laboratory of Living Donor Liver Transplantation, Ministry of Public Health, Department of Liver Transplantation Center, The First Affiliated Hospital of Nanjing Medical University, 300 Guangzhou Road, Nanjing 210029, Jiangsu, China

² Department of Oncological Surgery, Xuzhou City Central Hospital, The Affiliated Hospital of the Southeast University Medical School (Xu zhou), The Tumor Research Institute of the Southeast University (Xu zhou), 199 Jiefang South Road, Xuzhou 221009, Jiangsu, China

³ Department of Thoracic Surgery, Xuzhou City Central Hospital, The Affiliated Hospital of the Southeast University Medical School (Xu zhou), 199 Jiefang South Road, Xuzhou 221009, Jiangsu, China

⁴ Department of Gastroenterology 2, Xuzhou City Central Hospital, The Affiliated Hospital of the Southeast University Medical School (Xu zhou), 199 Jiefang South Road, Xuzhou 221009, Jiangsu, China

Abbreviations

| | |
|--------|-------------------------------|
| LC3-II | light chain 3-II |
| NCTD | norcantharidin |
| 3-MA | 3-methyladenine |
| HBSS | Hank's balanced salt solution |
| ROS | reactive oxygen species |

Introduction

Cholangiocarcinoma is a very common malignant tumor worldwide. Because of the insidious onset and higher malignancy of the disease, the cholangiocarcinoma treatment exhibits poor effectiveness [1–3]. Even surgical treatment is not particularly effective, and about 90% of patients are faced with recurrence and metastasis after surgery [4–6]. Accordingly, many scientists are putting great effort into developing more effective treatment methods or drugs for cholangiocarcinoma.

Traditional Chinese medicine exhibits a good curative effect for many diseases, it is also getting increasingly vital to cancer treatment [7–9]. Cantharidin, a Chinese patent medicine used for the treatment of tumors, refers to a terpenoid extracted from Chinese blister beetles. Norcantharidin (NCTD) is a synthetic cantharidin derivative that is adopted as an anticancer compound. NCTD is easy to synthesize and has broad anticancer applications in the treatment of liver cancer, colon cancer, leukemia, lung cancer, breast cancer, and cholangiocarcinoma [10–12].

Apoptosis refers to the stable and orderly death of cells controlled by genes to maintain the stability of the internal environment. Apoptosis is vital to the evolution of organisms and the development of multiple systems [13]. Many Chinese studies have reported that NCTD can accelerate apoptosis of cholangiocarcinoma cell lines. Our preliminary experiments were consistent with these studies. We have detected increased rates of apoptosis of the QBC939 and RBE cell lines treated with NCTD. Based on these preliminary studies and the work of other Chinese scholars, we decided to investigate NCTD effect on cholangiocarcinoma.

Autophagy is the processes by which organelles and other cytoplasmic materials are wrapped up by a double membrane vesicle (an autophagosome) for degradation [14, 15]. It was previously found that autophagy suppression up-regulates the antitumor effect of NCTD in hepatocellular carcinoma [16], and another study suggested that moderated autophagy will up-regulate the therapeutic activity of DNA-damage drugs towards intrahepatic cholangiocarcinoma [17]. These studies reveal the extraordinarily important role of autophagy in the survival of tumor cells, including cholangiocarcinoma.

Though the anticancer effects of both NCTD treatment and autophagy suppression in cholangiocarcinoma are known, the mechanism of NCTD-induced cytotoxic activity in cholangiocarcinoma remains unclear. This study aimed to characterize the association between NCTD and autophagy in the anticancer activity against cholangiocarcinoma. We hypothesized that the autophagy suppression would enhance Apoptosis induced NCTD in cholangiocarcinoma, and that the underlying molecular mechanism might involve mitochondrial apoptosis pathway activation.

Materials and Methods

Reagents and Materials

Gibco/Thermo Fisher Scientific, Inc. (Waltham, MA, USA) provided RPMI-1640 medium, penicillin, streptomycin, 10% heat-inactivated fetal bovine serum (FBS), and pancreatic enzymes. Sigma-Aldrich/Merck KGaA (Darmstadt, Germany) provided NCTD and Hank's balanced salt solution (HBSS). Roche Applied Science (Mannheim, Germany) provided Cell

Proliferation kit I (MTT). Primary antibodies, including β -actin (1/10000, ab227387), microtubule associated protein 1 light chain 3 (LC3-II) (1/3000, ab51520), caspase 3 (1/1000, ab2302), caspase 8 (1/1000, ab25901), caspase 9 (1/1000, ab32539), Bax (1/2000, ab32503). Bcl-2 (1/2000, ab182858) and cytochrome *c* (1/5000, ab133504). Secondary antibody, included goat Anti-Rabbit IgG horseradish peroxidase (1/4000, ab6721) and goat Anti-Mouse IgG horseradish peroxidase (1/4000, ab205719) were from Abcam (Cambridge, UK). Antibody against cleaved PARP was purchased from Santa Cruz Biotechnology, Inc. (1/500, sc-56,196, Santa Cruz, CA, USA). Beyotime (Haimen, China) provided the JC-1 dye mitochondrial membrane potential assay kit and radioimmunoprecipitation assay lysis buffer. The enhanced chemiluminescence (ECL) kit, protease inhibitor (Pierce Biotechnology, Rockford, IL, US), polyvinylidene difluoride membranes (Millipore, Bedford, MA, US). TRIzol reagent (Invitrogen, US), and PrimeScript RT Master Mix and SYBR Premix Ex Taq real-time PCR kit (Takara).

Cell Lines

The human cholangiocarcinoma cell line QBC939 was provided by the cell bank, Chinese Academy of Sciences (Shanghai, China) and cells were incubated in RPMI-1640 medium supported by 10% FBS, 50 U/ml streptomycin, and 50 U/ml penicillin at 37 °C in a 5% CO₂ humidified environment.

Cell Treatments

QBC939 cells were split into 8 treatment groups: 1) Sham group cells incubated in RPMI-1640 medium. 2) NCTD group cells incubated in RPMI-1640 medium that contained NCTD (0, 0.01, 0.02, 0.04, 0.08, or 0.16 mM) for 24 h [10]. 3) HBSS group cells were first cultured in HBSS media with Ca²⁺ and Mg²⁺ supported by 10 mM HEPES (1 ml/well) for 0.5 h to induce autophagy [18], and then cleaned with PBS twice, followed by culturing in RPMI-1640 medium for 24 h. 4) HBSN (HBSS+NCTD) group cells were first cultured in HBSS media with Ca²⁺ and Mg²⁺ supported by 10 mM HEPES (1 ml/well), and then cleaned with PBS twice, followed by culturing in RPMI-1640 medium that contained NCTD (0.16 mM) for 24 h. 5) 3-MA group cells incubated in RPMI-1640 medium that contained 3-MA (10 mM) [19]. 6) 3-MAN (3-MA + NCTD) group cells were first cultured in RPMI-1640 medium that contained 3-MA (10 mM) to inhibit autophagy, then cleaned twice with PBS, followed by culturing in RPMI-1640 medium that contained NCTD (0.16 mM) for 24 h. 7) SS group cells were transfected with Atg5-siRNA and cultured in RPMI-1640 medium. 8) SSN (Atg5-siRNA+

NCTD) group cells were transfected with Atg5-siRNA and incubated in RPMI-1640 medium, then cleaned 2 times with PBS, followed by culturing in RPMI-1640 medium that contained NCTD (0.16 mM) for 24 h.

MTT Assay

Cells were incubated in 96-well flat bottom microtiter plates at 1×10^4 cells/well overnight and treated with NCTD (0–0.3 mM) at different concentrations the following day. Subsequently, the cells underwent the incubation with MTT (20 μ l) solution (5 g/l) for 4 h at 37 °C. For the calculation of the absorbance value per well at 570 nm, an automatic multi-well spectrophotometer was used. Every MTT assay was conducted 3 times. The cell viability ratio was calculated by: cell viability (%) = average absorbance of treated group / average absorbance of sham group \times 100%. Next, with the use of the Statistical Package for the Social Sciences 17.0 (SPSS, Inc., Chicago, IL, USA), IC50 values (50% inhibition concentration) were calculated.

Small Interfering RNA (siRNA) Transfection

Ambion (Austin, TX, US) provided small interfering RNAs (siRNAs) against Atg5 and a nonspecific scrambled siRNA. All siRNAs were yielded by Qiagen (Chatsworth, CA, US). QBC939 cells underwent incubation in 6-well plates. Lipofectamine 2000 (Invitrogen, Rockville, MD, US) was intermingled into RPMI-1640 medium without FBS that contained siRNA1, siRNA2, or scrambled siRNA. Mock controls were transfected with Lipofectamine 2000 (Invitrogen) alone. Transfection was performed at 37 °C in a 5% CO₂ humidified atmosphere, then serum that contained medium replaced with the medium for 4–6 h. Cells underwent the treatment as presented below after 2 h [16].

RNA Extraction and Reverse Transcription Quantitative Real-Time PCR

With the use of TRIzol, Total RNA was isolated and purified, and cDNA was formed by the PrimeScript RT Master Mix. We used 2 μ l cDNA as a template in a 20- μ l reaction. Primers were yielded by Invitrogen (Shanghai, China). Atg5 primers were 5'-TTCTCAAATATACTGTTTC-3' (sense) and 5'-TATTATGTATCACAATGG-3' (antisense). β -actin primers were 5'-TCACCCACACTGTGCCCATCTACGA-3' (sense) and 5'-CAGCGGAACCGCTCATTGCCAATGG-3' (antisense). PCR was conducted under 95 °C for 30 s; 40 cycles of 95 °C for 5 s and 60 °C for 31 s; and 95 °C for 15 s, 60 °C for 1 min, and 95 °C for 15 s.

Western Blotting Analysis

Protein was extracted from human cholangiocarcinoma cells using Cell Lysis Reagents (Pierce), and with the use of the BCA protein assay, protein concentrations were quantified. To detect cytochrome c, cells were sonicated in buffer that contained 10 mM Tris-HCl pH 7.5, 10 mM NaCl, 175 mM sucrose, and 12.5 mM EDTA, and then centrifuged at 1000 g for 10 min to pellet nuclei. The supernatant was then centrifuged at 18000 g for 30 min to pellet the mitochondria and purified. The resulting supernatant was termed the cytosolic fraction. [10, 20]. Next, the proteins were separated on a 10% SDS-polyacrylamide gel and transferred to a polyvinylidene difluoride membrane. The membrane was then incubated with the primary antibodies with shaking at 4 °C overnight, then incubated with secondary antibody at 37 °C for 1 h. Finally, the membrane was visualized using an ECL detection kit. The band intensities were measured by Image-Pro Plus 6.0.

Immunofluorescence

Cells fixed on coverslips underwent incubation in 4% paraformaldehyde for 20 min. Cells were then blocked in 10% BSA for 1 h and incubated with the primary antibody at 4 °C overnight, followed by incubation with secondary antibody for 1 h at 37 °C the next day. Cells were incubated with 4',6-diamidino-2-phenylindole and monitored by confocal microscopy to detect autophagy. Ten visual fields were chosen randomly, and the optical density was measured by Image-Pro Plus 6.0.

Analysis of Reactive Oxygen Species (ROS) Production

The ROS level was detected by flow cytometry using DCHF-DA. Cells were cleaned with D-Hank's solution three times, and then were cultured in RPMI-1640 medium without FBS that contained DCHF-DA (100 μ M) in dark at 37 °C for 30 min. After that, cells were cleaned with RPMI-1640 medium without FBS and then treated with pancreatic enzymes. DCF fluorescence was detected at an emission wavelength of 525 nm and an excitation wavelength of 488 nm.

Annexin-V/PI Staining Assay

Apoptosis was detected in QBC939 cells with the use of the Annexin-V-FITC kit. After washing twice with ice-cold PBS, the cells were resuspended in 400 μ l binding buffer to a concentration of 5×10^5 cells/ml. The cells were treated with 5 μ l of Annexin-V-FITC and 5 μ l of PI, vortexed, and cultured in dark at 4 °C. Subsequently, apoptosis was analyzed by FACS Calibur flow cytometer (BD, San Jose, CA, USA) using Cell Quest software (BD).

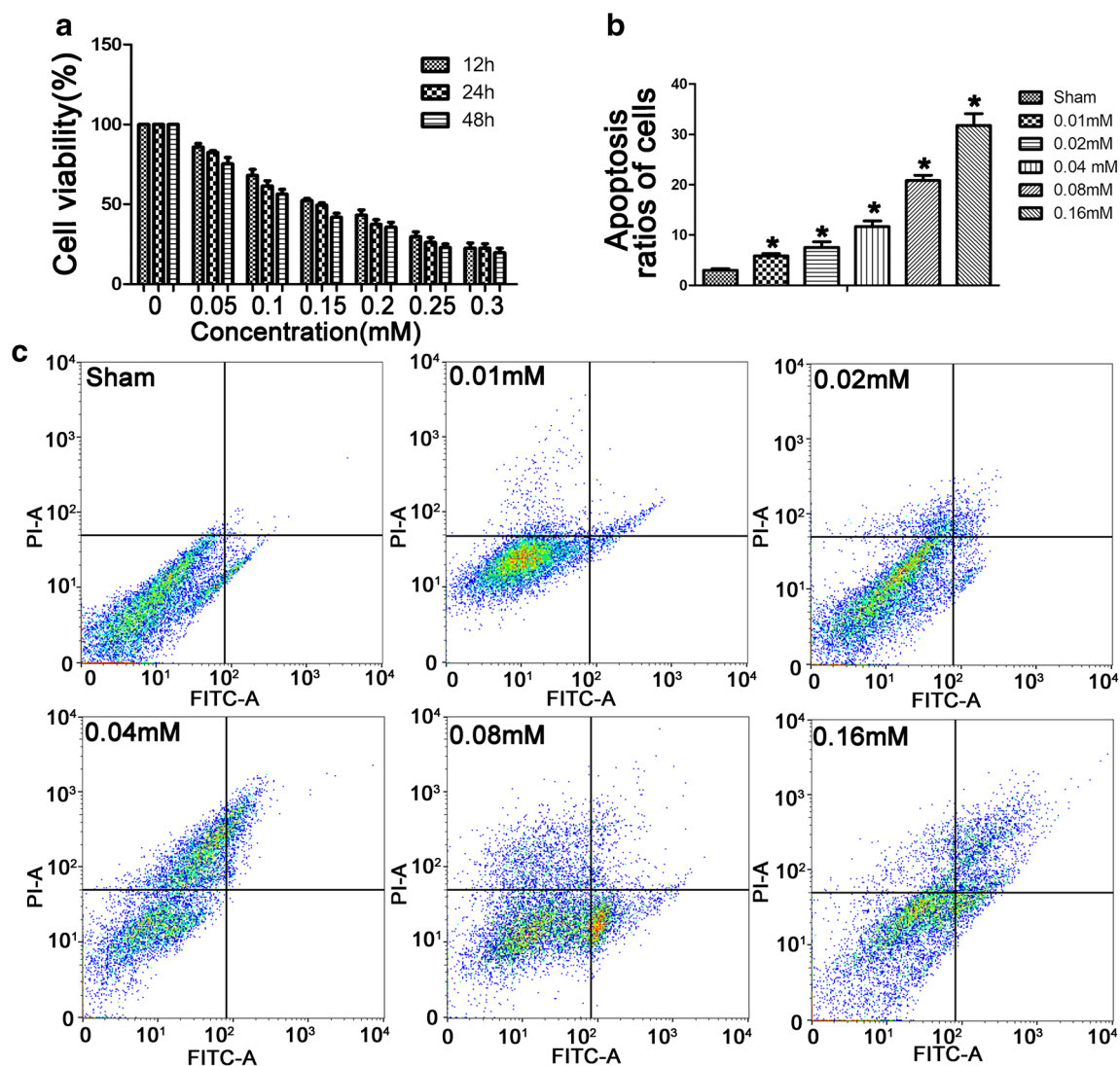


Fig. 1 NCTD induced apoptosis in the QBC939 cell line. **a** QBC939 cells were treated with 0–0.3 mM NCTD for 12, 24 or 48 h and proliferation was assessed with the MTT assay. **b, c** NCTD increased the apoptotic cell ratios in a dose-dependent manner. * $p < 0.05$ compared with the sham group

Mitochondrial Membrane Potential ($\Delta\Phi_m$) Assay

The mitochondrial membrane potential was monitored by JC-1 assay. The cells underwent the treatment with JC-1 dyeing liquid (1 ml/well) and incubation at 37 °C for 20 min. The cells were cleaned twice with 1× dyeing buffer, followed by culturing in RPMI-1640 medium. Cells were observed by fluorescence microscopy (AX10, Carl Zeiss, Hamburg, Germany).

Statistical Analysis

The data are denoted as mean \pm standard deviation. Statistical analysis was conducted by ANOVA and Dunnett test. Multiple comparisons between the groups were drawn using S-N-K method after ANOVA. SPSS17.0 software was applied for

all statistical analyses, and a P value < 0.05 was considered statically significant.

Results

NCTD Inhibits QBC939 Cell Proliferation and Induces Caspase-Mediated Apoptosis

The results of MTT assay suggested that NCTD suppressed the proliferation QBC939 cells in a dose- and time-dependent manner after treatment with 0–0.3 mM NCTD for 12, 24, or 48 h (Fig. 1a). At concentrations higher than 0.01 mM, NCTD treatment significantly suppressed cell proliferation. The IC50 value of NCTD treatment at 24 h was 0.16 mM. Thus, a range

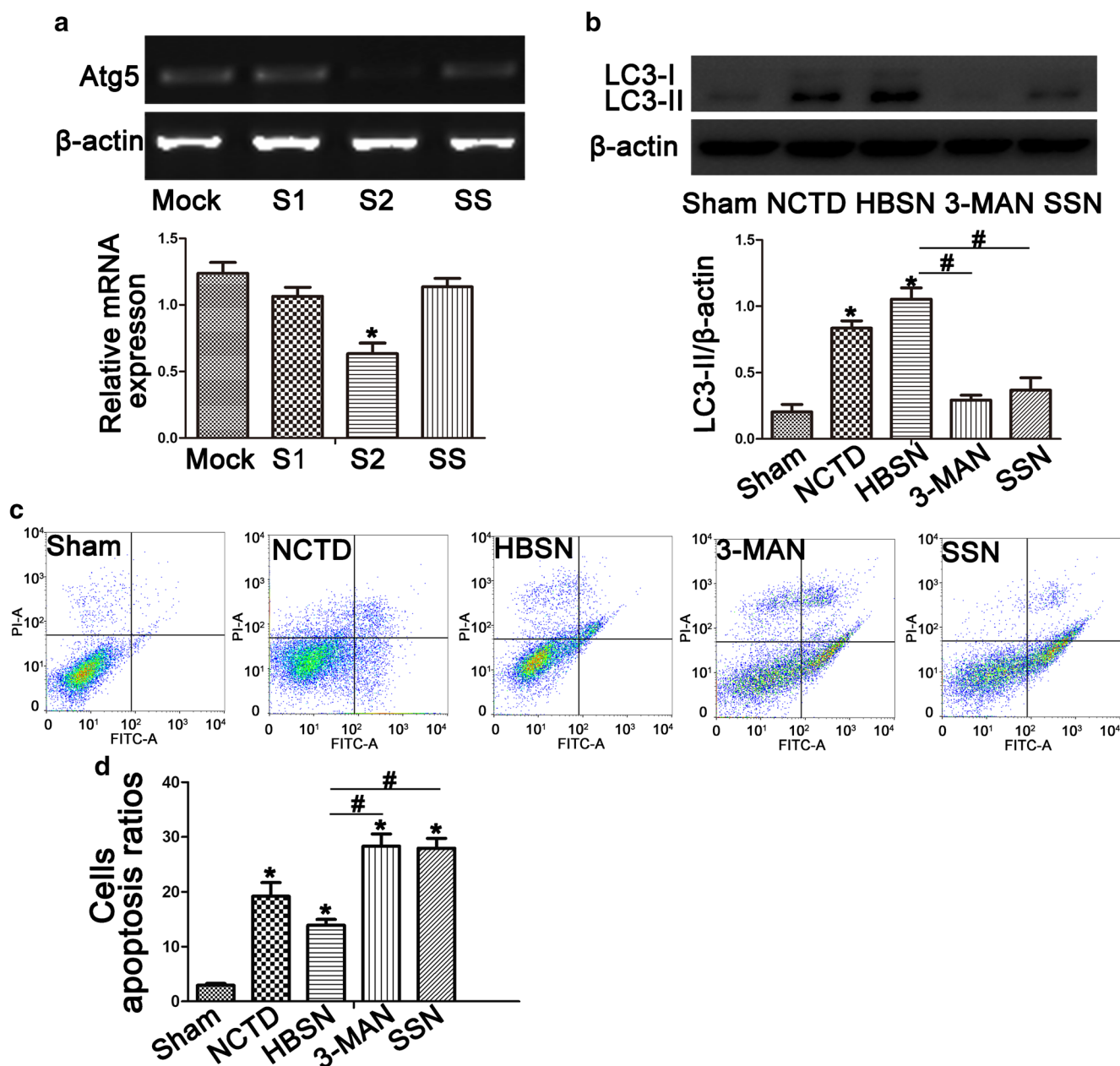


Fig. 2 Inhibition of autophagy induced apoptosis in the QBC939 cell line. **a** Decreased expression of Atg5 was confirmed by RT-qPCR in the Atg5 siRNA-transfected and NCTD-treated cells compared with the Mock group (S1: with siRNA1, S2: with siRNA2, SS: with scrambled RNA. * $p < 0.05$ compared with the sham group). **b** Western blotting showed LC3-II protein expression was increased in the HBSN group

(HBSN+NCTD), whereas LC3-II expression was inhibited by 3-MA and Atg5 siRNA. **c, d** Annexin-V/PI staining showed that the cell apoptosis ratios decreased in the autophagy up-regulation group (HBSN) and increased in the autophagy down-regulation group. * $p < 0.05$ compared with the sham group; # $p < 0.05$ compared with the HBSN group

of concentrations (0, 0.01, 0.02, 0.04, 0.08 and 0.16 mM) was applied, and the concentration of 0.16 mM was used for all subsequent experiments.

NCTD Induced Apoptosis in the QBC939 Cell Line

QBC939 cells showed up-regulated ratios of apoptotic to total cells when treated with NCTD, and this increase

was dose-dependent. The sham group had $2.95 \pm 0.76\%$ apoptotic cells, which were up-regulated to $5.82 \pm 1.0\%$, $7.5 \pm 2.46\%$, $11.66 \pm 2.52\%$, $20.83 \pm 2.4\%$, or $31.79 \pm 5.29\%$ by the treatment with 0.01, 0.02, 0.04, 0.08 and 0.16 mM NCTD, respectively (Fig. 1). This result has consistency with our previous findings, so the 10 $\mu\text{g/ml}$ dose was selected for use in all subsequent experiments.

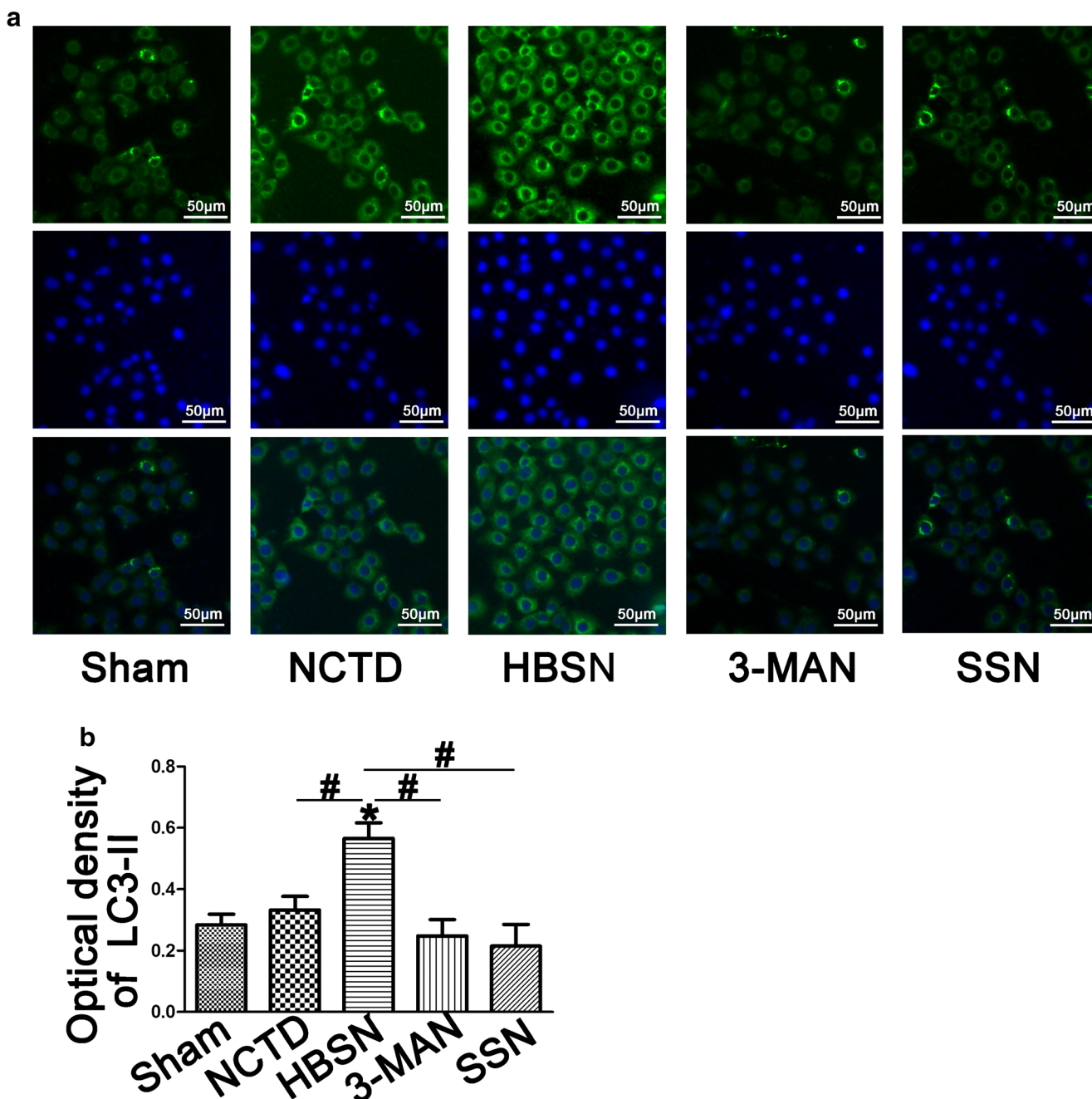


Fig. 3 Inhibition of autophagy was confirmed by decreased levels of the LC3-II protein. (A, B) Immunofluorescence microscopy showed decreased LC3-II staining in the autophagy inhibition (3-MA and Atg5-

siRNA) groups, but LC3-II levels increased when autophagy was induced (HBSN group). * $p < 0.05$ compared with the sham group; # $p < 0.05$ compared with the HBSN group

Up-Regulation of Autophagy Decreased Apoptosis Induced NCTD

Autophagy was triggered in QBC939 cells by HBSS, which was verified by greater LC3-II protein expression detected by western blotting and immunostaining (Fig. 2b, Fig. 3, $P < 0.05$). It is noteworthy that the rates of early and late apoptosis induced by NCTD, as detected by Annexin-V/PI staining, were lower in cells treated with HBSS before NCTD addition

(HBSN group) compared with either the sham or NCTD groups (Fig. 2c, both $P < 0.05$).

Autophagy Suppression Induced Apoptosis

Autophagy was suppressed by 3-MA or siRNA against Atg5. The decreased gene expression of Atg5 in the Atg5-siRNA (SSN) group compared with the sham group was verified by RT-qPCR (Fig. 2a, $P < 0.05$), and reduced LC3-II expression

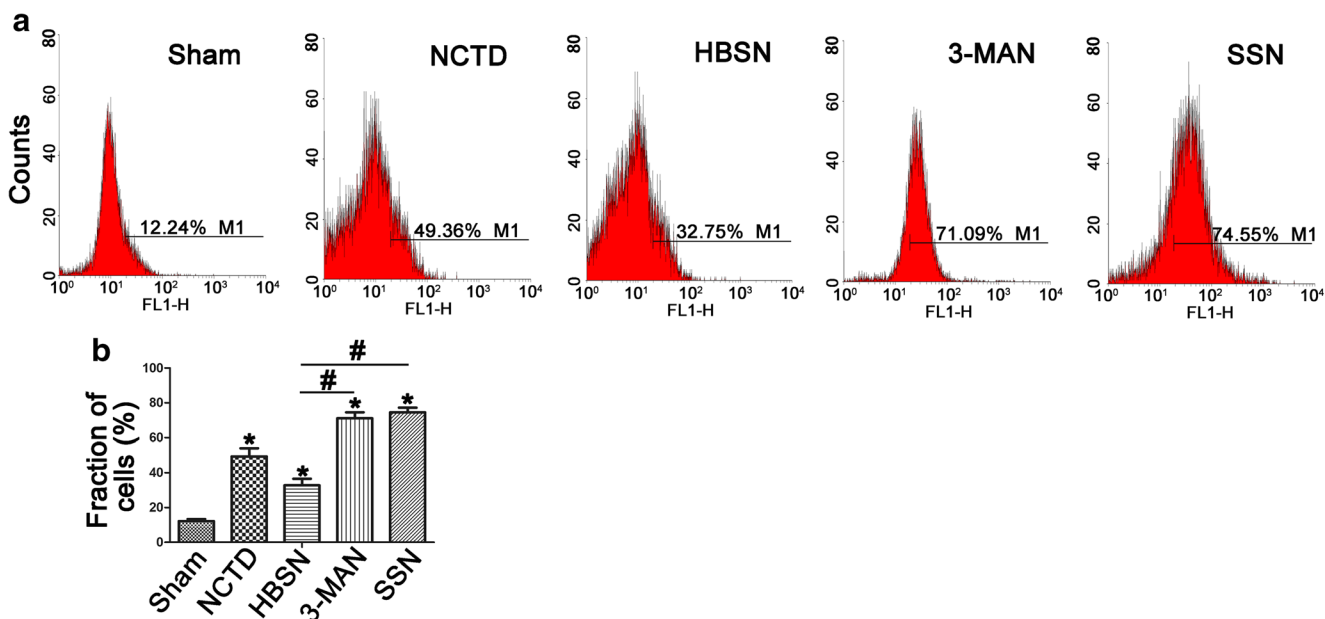


Fig. 4 Inhibition of autophagy enhanced NCTD-induced ROS generation. **a, b** Increasing intracellular ROS generation was observed in the NCTD group. Inhibition of autophagy further enhanced ROS

generation compared with the NCTD group, and induction of autophagy decreased ROS levels. * $p < 0.05$ compared with the sham group; # $p < 0.05$ compared with the HBSN group

was verified in the 3-MAN and Atg5-siRNA (SSN) groups compared with the sham group by western blotting and immunostaining (Fig. 2b, Fig. 3, $P < 0.05$). Apoptosis increased in both the 3-MAN and Atg5-siRNA groups (Fig. 2c, $P < 0.05$).

Autophagy Suppression Enhanced ROS Generation Induced by NCTD

Intracellular ROS levels were higher in the NCTD group than in the sham group, and autophagy suppression further promoted ROS generation induced by NCTD in the 3-MAN and Atg5-siRNA (SSN) groups when compared with the NCTD group. Conversely, when autophagy was induced in the HBSN group, the ROS level was down-regulated compared with the NCTD group (Fig. 4a, b).

Autophagy Suppression Induces pro-Apoptotic Protein Expression

Autophagy suppression in the 3-MAN and SSN group increased the Bax and Cytosol cytochrome c protein compared with the sham and NCTD group, which was adverse when autophagy was induced in the HBSN group ($P < 0.05$). But the autophagy suppression reduced the mitochondrial cytochrome c and Bcl-2 protein expression compared with the sham and NCTD group (Fig. 5, $P < 0.05$).

Elevated cleaved caspase 3 and cleaved caspase 9 levels were detected when autophagy was suppressed in cell line QBC939; however, this increase was abrogated in the HBSN group (all $P < 0.05$). No significant variations in

caspase-8 protein expression were observed between any groups. Autophagy suppression in cell line QBC939 also promoted the cleavage of PARP (poly (ADP-ribose) polymerase) protein from the full-length form to the cleaved form (Fig. 6, $P < 0.05$).

More Mitochondrial Membrane Potential Disturbance Was Observed under Autophagy Suppression Conditions

More red fluorescence was present in the sham and HBSN groups, and more green fluorescence in the 3-MAN and Atg5-siRNA (SSN) groups. The higher green fluorescence in these cells is considered to reveal more mitochondrial membrane potential disturbance (Fig. 7a, b, $P < 0.05$).

Discussion

Cholangiocarcinoma is one of the leading causes of cancer mortality worldwide, considered incurable and lethal because the majority of these tumors cannot be fully resected, and thus many cases are only treated with palliative chemotherapy and radiotherapy to improve the quality of life and extend survival in patients [21]. The significant side effects of chemoradiotherapy and the high mortality of cholangiocarcinoma lay the foundation for the discovery of novel treatments for cholangiocarcinoma with fewer side effects [22].

In China, NCTD is a synthetic analog of the Chinese patent medicine cantharidin widely used for cancer treatment [10–12]. N-hydroxycantharidin, which is also synthesized

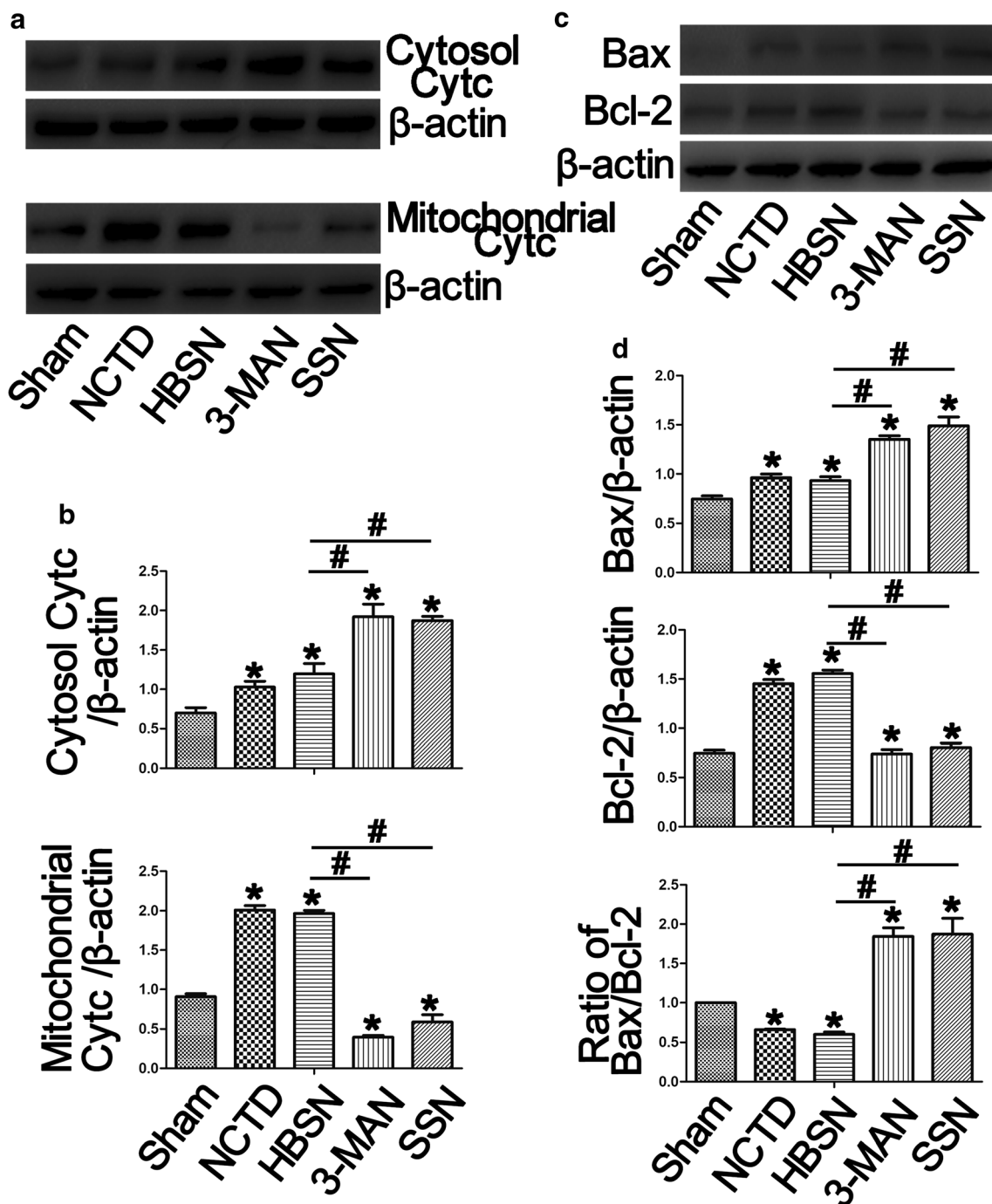


Fig. 5 Inhibition of autophagy induced Bax and cytosolic cytochrome c protein expression and reduced Bcl-2 expression. **a, b** The cytosolic expression of cytochrome c protein was significantly increased and the mitochondrial expression was decreased when autophagy was down-regulated, but the increase was abrogated when autophagy was induced in the HBSN group (HBSS+NCTD). **c, d** Bax protein expression was up-

regulated in the 3-MAN (3-MA + NCTD) and Atg5-siRNA-N (Atg5 siRNA+NCTD) groups compared with the sham and HBSN (HBSS+NCTD) groups, but the Bcl-2 protein was more highly expressed in the HBSN group. The ratio of Bax/Bcl-2 was more higher in the autophagy inhibition group. * $p < 0.05$ compared with the sham group; # $p < 0.05$ compared with the HBSN group

from cantharidin, has shown curative effects in certain tumors [7, 17]. NCTD and cantharidin both have been reported to play a potent anticancer role by activating the apoptosis pathway in various cancer cells. Therefore, we examined the cytotoxic effects of NCTD on the cell line QBC939 and found that NCTD increased apoptosis ratios, which has consistency

with the previous study and our speculation. We further found that the NCTD-induced increase in apoptotic ratios was dose dependent.

Autophagy, a process in which cytoplasmic macromolecules or organelles are degraded in lysosomes to maintain balance in the cell, is activated by environmental stress to

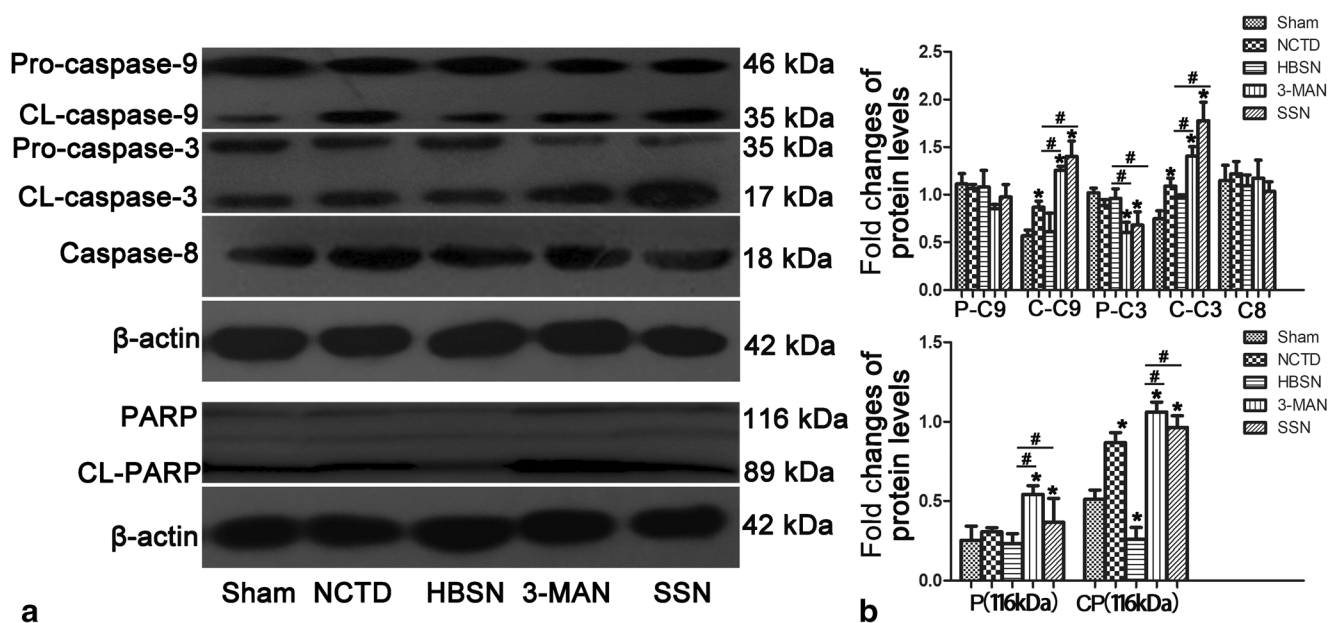


Fig. 6 Inhibition of autophagy in the QBC939 cell line increased levels of cleaved caspase-3, caspase-9, and PARP. **a, b** More cleaved caspase-3 and -9 proteins were detected when autophagy was inhibited, but the increase was abrogated in the HBSN group. Caspase-8 protein expression did not differ between groups. More of the cleaved form of the PARP protein (89 kDa) was detected in the 3-MAN (3-MA + NCTD)

and Atg5-siRNA-N (Atg5 siRNA+NCTD) groups in which autophagy was reduced, and more full-length PARP protein (116 kDa) was detected in the HBSN (HBSN+NCTD) group. P-C9: pro-caspase-9; C-C9: CL-caspase-9; P-C3: pro-caspase-3; C-C3: CL-caspase-3; C8: Caspase-8; * $p < 0.05$ compared with the sham group; # $p < 0.05$ compared with the HBSN group

promote cell survival; however, autophagy appears to promote cell death and morbidity in other contexts [23–26]. Additionally, many studies found a key role of autophagy in tumor cells by demonstrating that the autophagy suppression in cholangiocarcinoma enhances sensitivity to chemotherapy [17]. Most interestingly, we found in the present study that and the pro-apoptotic effect of NCTD is enhanced by the down-regulation of autophagy, which is in accordance with previous research. However, the specific association between autophagy and the mechanism of action of NCTD require further study.

Apoptosis is divided into the extrinsic death receptor-mediated pathway and intrinsic mitochondria-mediated pathway [27, 28]. Many studies verified the drug-induced apoptosis effects of Chinese patent medicines, including NCTD, and reported that NCTD could effectively treat cancer via accelerating mitochondria-mediated apoptosis pathway activation [29, 30]. Note that one form of autophagy is the degradation of mitochondria in a process termed mitophagy [31]. Thus, based on the research above, we focused on the proteins involved in these apoptotic pathways. Bax, a pro-apoptotic protein, and Bcl-2, an anti-apoptotic protein, are vital to induce mitochondrial death cascade [32]. We found that induction of autophagy in the cell line QBC939 reduced Bax protein expression but up-regulated Bcl-2 protein expression. However, the autophagy suppression in cells increased Bax protein expression but down-regulated Bcl-2 protein expression.

Additionally, the levels of cytosolic cytochrome c protein were increased, and the levels of mitochondrial cytochrome c protein were decreased in the autophagy down-regulation groups, whereas the effect was reversed in the autophagy up-regulation group. We also detected caspase-3, -8, and -9 proteins, because the activation of caspase-3 and caspase-9 proteins is vital to the mitochondrial apoptotic pathway [33]. The cleaved caspase-3 and -9 proteins levels were up-regulated when autophagy was suppressed and reduced when autophagy was induced. We found no variations of incaspase-8 protein expression between any of the groups.

We next analyzed cleavage of the PARP protein, being vital to the apoptotic pathway and cleaved by activated caspase-3. Greater levels of cleaved (89 kDa) PARP protein were detected in the 3-MAN and Atg5-siRNA groups in which autophagy was reduced, whereas we detected more full-length (116 kDa) PARP protein in the HBSN group in which autophagy was induced. This verified our hypothesis and previous results. Besides, the mitochondrial membrane potential in cells was examined using a fluorescent dye. We observed more green fluorescence, suggesting mitochondrial membrane potential disturbance, in the groups with down-regulated autophagy (3-MAN and Atg5-siRNA). Combined with the results described above, we assumed that the autophagy suppression in QBC939 cells accelerated apoptosis induced NCTD via, at least in part, mitochondrial apoptotic pathway activation.

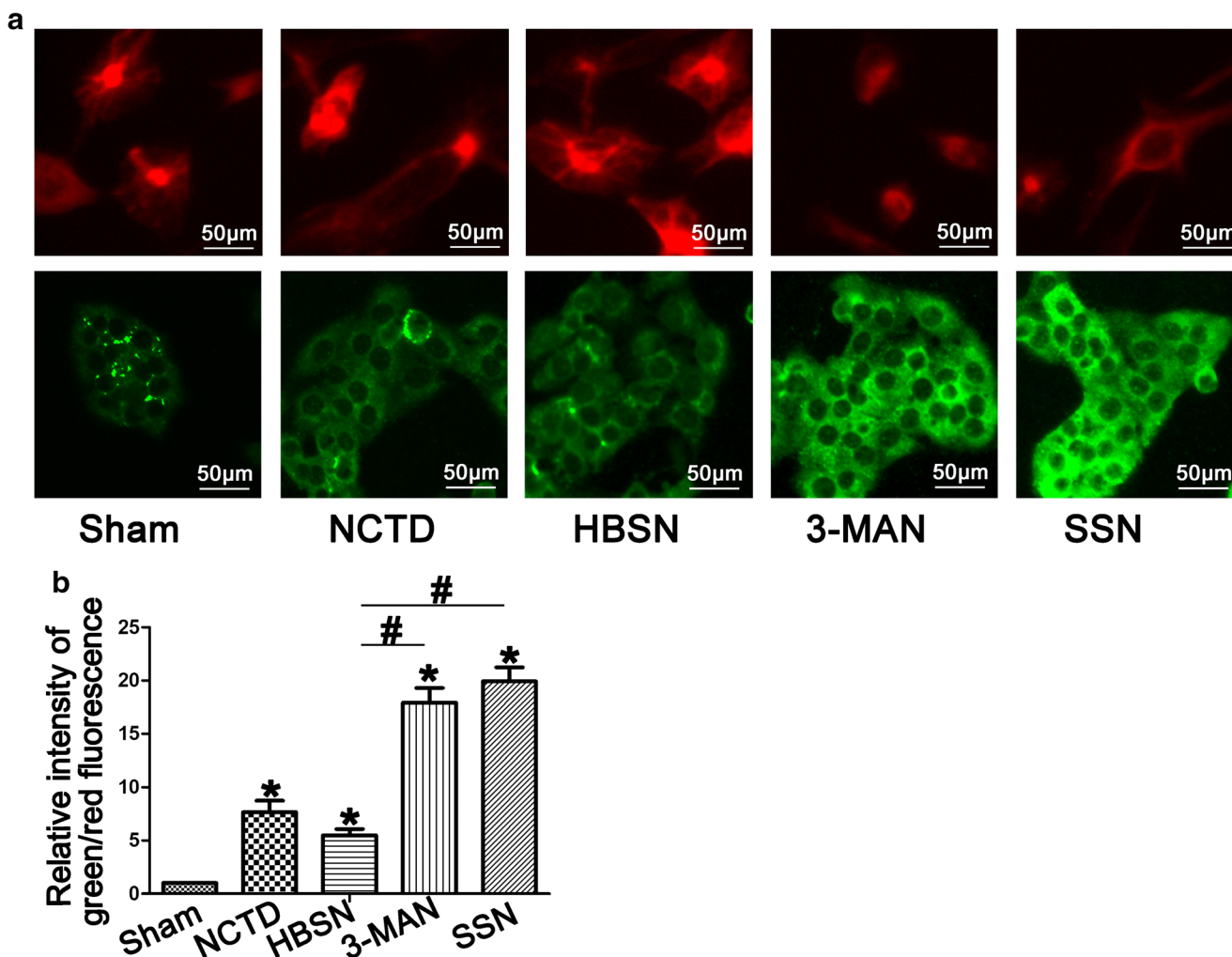


Fig. 7 Mitochondrial membrane potential was more disrupted when autophagy was inhibited in the QBC939 cell line. **a, b** The increased green fluorescence in the 3-MAN (3-MA + NCTD) and Atg5-siRNA-N (Atg5 siRNA+NCTD) groups cells represented more mitochondrial

membrane potential disturbance, whereas the red fluorescence in the sham and HBSN (HBSN+NCTD) groups represented less disturbance. * $p < 0.05$ compared with the sham group; # $p < 0.05$ compared with the HBSN group

ROS are generated during metabolic processes, and they are vital to tumor occurring, developing and recurring process. The generation of ROS can promote mitochondrial membrane potential disturbance, which leads to cell death, thus serving as an apoptotic signaling molecule [29, 30, 32]. In our study, we found that NCTD could increase intracellular ROS generation, and autophagy suppression further promoted ROS generation induced by NCTD. Conversely, ROS generation decreased when autophagy was induced.

In the present study, we demonstrated that NCTD could trigger apoptosis in the cell line QBC939 through mitochondrial apoptotic pathway activation and ROS generation, and autophagy suppression accelerated this Apoptosis induced NCTD. The association between the mitochondrial apoptotic pathway and autophagy in cholangiocarcinoma cells requires further study, which could lead to the development of new therapies against this cancer or others.

Acknowledgments The study was financed by grants from the National Science Foundation of China (81670570), Key research and development program of Jiangsu Province (BE2016789).

Authors' Contributions YW, XL, WJ, CJ and XX conception and design, or analysis and interpretation of data; YW, WJ, CJ, XX, HG and QT drafting the article; XL is the guarantor for the article.

Compliance with Ethical Standards

Conflict of Interest No conflict of interest was declared by the authors.

References

- Walden D, Kunnimalaiyaan S, Sokolowski K, Clark TG, Kunnimalaiyaan M (2017) Antiproliferative and apoptotic effects of xanthohumol in cholangiocarcinoma. *Oncotarget* 8:88069–88078

2. Guan L, Zhang L, Gong Z, Hou X, Xu Y, Feng X, Wang H, You H (2016) FoxO3 inactivation promotes human cholangiocarcinoma tumorigenesis and chemoresistance through Keap1-Nrf2 signaling. *Hepatology* 63:1914–1927
3. Zhang H, Yang T, Wu M, Shen F (2016) Intrahepatic cholangiocarcinoma: epidemiology, risk factors, diagnosis and surgical management. *Cancer Lett* 379:198–205
4. Hu MH, Chen LJ, Chen YL, Tsai MS, Shiau CW, Chao TI, Liu CY, Kao JH, Chen KF (2017) Targeting SHP-1-STAT3 signaling: a promising therapeutic approach for the treatment of cholangiocarcinoma. *Oncotarget* 8:65077–65089
5. Roskoski R Jr (2017) ROS1 protein-tyrosine kinase inhibitors in the treatment of ROS1 fusion protein-driven non-small cell lung cancers. *Pharmacol Res* 121:202–212
6. Thanee M, Loilome W, Techasen A, Sugihara E, Okazaki S, Abe S, Ueda S, Masuko T, Namwat N, Khuntikeo N, Titapun A, Pairojkul C, Saya H, Yongvanit P (2016) CD44 variant-dependent redox status regulation in liver fluke-associated cholangiocarcinoma: a target for cholangiocarcinoma treatment. *Cancer Sci* 107:991–1000
7. Wang X, Yu S, Jia Q, Chen L, Zhong J, Pan Y, Shen P, Shen Y, Wang S, Wei Z, Cao Y, Lu Y (2017) NiaoDuQing granules relieve chronic kidney disease symptoms by decreasing renal fibrosis and anemia. *Oncotarget* 8:55920–55937
8. Fu H, Wu R, Li Y, Zhang L, Tang X, Tu J, Zhou W, Wang J, Shou Q (2016) Safflower yellow prevents pulmonary metastasis of breast Cancer by inhibiting tumor cell Invadopodia. *Am J Chin Med* 44:1491–1506
9. Xiao W, Wu K, Yin M, Han S, Ding Y, Qiao A, Lu G, Deng B, Bo P, Gong W (2015) Wogonin inhibits tumor-derived regulatory molecules by suppressing STAT3 signaling to promote tumor immunity. *J Immunother* 38:167–184
10. Chang C, Zhu YQ, Mei JJ, Liu SQ, Luo J (2010) Involvement of mitochondrial pathway in NCTD-induced cytotoxicity in human hepG2 cells. *J Exp Clin Cancer Res* 29:145
11. Han W, Wang S, Liang R, Wang L, Chen M, Li H, Wang Y (2013) Non-ionic surfactant vesicles simultaneously enhance antitumor activity and reduce the toxicity of cantharidin. *Int J Nanomedicine* 8:2187–2196
12. Yeh CB, Su CJ, Hwang JM, Chou MC (2010) Therapeutic effects of cantharidin analogues without bridging ether oxygen on human hepatocellular carcinoma cells. *Eur J Med Chem* 45:3981–3985
13. Sakahira H, Enari M, Nagata S (2015) Corrigendum: cleavage of CAD inhibitor in CAD activation and DNA degradation during apoptosis. *Nature* 526:728
14. Rautou PE, Mansouri A, Lebre C, Durand F, Valla D, Moreau R (2010) Autophagy in liver diseases. *J Hepatol* 53:1123–1134
15. Moretti J, Roy S, Bozec D, Martinez J, Chapman JR, Ueberheide B et al (2017) STING senses microbial viability to orchestrate stress-mediated autophagy of the endoplasmic reticulum. *Cell* 171 e13:809–823
16. Xiong X, Wu M, Zhang H, Li J, Lu B, Guo Y et al (2015) Atg5 SiRNA inhibits autophagy and enhances norcantharidin-induced apoptosis in hepatocellular carcinoma. *Int J Oncol* 47:1321–1328
17. Hou YJ, Dong LW, Tan YX, Yang GZ, Pan YF, Li Z, Tang L, Wang M, Wang Q, Wang HY (2011) Inhibition of active autophagy induces apoptosis and increases chemosensitivity in cholangiocarcinoma. *Lab Invest* 91:1146–1157
18. Settembre C, Di Malta C, Polito VA, Garcia Arencibia M, Vetrini F, Erdin S et al (2011) TFEB links autophagy to lysosomal biogenesis. *Science* 332:1429–1433
19. Carchman EH, Rao J, Loughran PA, Rosengart MR, Zuckerbraun BS (2011) Heme oxygenase-1-mediated autophagy protects against hepatocyte cell death in hepatic injury from infection/sepsis in mice. *Hepatology* 53:2053–2062
20. Lewis JS, Meeke K, Osipo C, Ross EA, Kidawi N, Li T, Bell E, Chandel NS, Jordan VC (2005) Intrinsic mechanism of estradiol-induced apoptosis in breast cancer cells resistant to estrogen deprivation. *J Natl Cancer Inst* 97:1746–1755
21. Mavros MN, Economopoulos KP, Alexiou VG, Pawlik TM (2014) Treatment and prognosis for patients with intrahepatic cholangiocarcinoma: systematic review and meta-analysis. *JAMA Surg* 149:565–574
22. Lau SH, Lau WY (2012) Current therapy of hilar cholangiocarcinoma. *Hepatobiliary Pancreat Dis Int* 11:12–17
23. Estrabaud E, De Muynck S, Asselah T (2011) Activation of unfolded protein response and autophagy during HCV infection modulates innate immune response. *J Hepatol* 55:1150–1153
24. Tai H, Wang Z, Gong H, Han X, Zhou J, Wang XN et al (2017) Autophagy impairment with lysosomal and mitochondrial dysfunction is an important characteristic of oxidative stress-induced senescence. *Autophagy* 13:99–113
25. Toshima T, Shirabe K, Fukuhara T, Ikegami T, Yoshizumi T, Soejima Y, Ikeda T, Okano S, Maehara Y (2014) Suppression of autophagy during liver regeneration impairs energy charge and hepatocyte senescence in mice. *Hepatology* 60:290–300
26. Whitehead NP (2016) Enhanced autophagy as a potential mechanism for the improved physiological function by simvastatin in muscular dystrophy. *Autophagy* 12:705–706
27. Xie SQ, Zhang YH, Li Q, Xu FH, Miao JW, Zhao J, Wang CJ (2012) 3-nitro-naphthalimide and nitrogen mustard conjugate NNM-25 induces hepatocellular carcinoma apoptosis via PARP-1/p53 pathway. *Apoptosis* 17:725–734
28. Qi F, Inagaki Y, Gao B, Cui X, Xu H, Kokudo N et al (2012) Bufalin and cinobufagin induce apoptosis of human hepatocellular carcinoma cells via Fas- and mitochondria-mediated pathways. *Cancer Sci* 102:951–958
29. Shen B, He PJ, Shao CL (2013) Norcantharidin induced DU145 cell apoptosis through ROS-mediated mitochondrial dysfunction and energy depletion. *PLoS One* 8:e84610
30. Zhao L, Yang G, Bai H, Zhang M, Mou D (2017) NCTD promotes Birinapant-mediated anticancer activity in breast cancer cells by downregulation of c-FLIP. *Oncotarget* 8:26886–26895
31. Fang EF, Scheibye-Knudsen M, Brace LE, Kassahun H, SenGupta T, Nilsen H, Mitchell JR, Croteau DL, Bohr VA (2014) Defective mitophagy in XPA via PARP-1 hyperactivation and NAD(+)/SIRT1 reduction. *Cell* 157:882–896
32. Choi BM, Chen XY, Gao SS, Zhu R, Kim BR (2011) Anti-apoptotic effect of phloretin on cisplatin-induced apoptosis in HEI-OC1 auditory cells. *Pharmacol Rep* 63:708–716
33. Prenek L, Boldizsár F, Kugyelka R, Ugor E, Berta G, Németh P, Berki T (2017) The regulation of the mitochondrial apoptotic pathway by glucocorticoid receptor in collaboration with Bcl-2 family proteins in developing T cells. *Apoptosis* 22:239–253